

AutoFT: Learning an Objective for Robust Fine-Tuning

Caroline Choi^{*1} Yoonho Lee^{*1} Annie Chen¹ Allan Zhou¹ Aditi Raghunathan² Chelsea Finn¹

Abstract

Foundation models encode rich representations that can be adapted to downstream tasks by fine-tuning. However, fine-tuning a model on one data distribution often degrades performance under distribution shifts. Current approaches to robust fine-tuning use hand-crafted regularization techniques to constrain the fine-tuning process towards the pretrained model. Yet, it is hard to specify how to adapt relevant characteristics of the foundation model during fine-tuning, as this depends on how the pre-training, fine-tuning, and test data distributions relate to each other. We propose AUTOFT, a data-driven approach for robust fine-tuning. Given a task, AUTOFT searches for a fine-tuning procedure that enhances out-of-distribution (OOD) generalization. Specifically, AUTOFT uses bi-level optimization to search for an objective function and hyperparameters that maximize post-adaptation performance on a small OOD validation set. We evaluate AUTOFT on nine natural distribution shifts. Our experiments show that AUTOFT significantly improves generalization to OOD inputs, outperforming existing robust fine-tuning methods. Notably, AUTOFT achieves a new state-of-the-art on the WILDS iWildCam and FMoW benchmarks, outperforming the previous best methods by 6.0% and 1.5%, respectively.

1 Introduction

Foundation models have emerged as a powerful tool in machine learning, demonstrating unprecedented performance across a wide variety of data distributions (Radford et al., 2021b; Ilharco et al., 2021; Jia et al., 2021). By pre-training on large and diverse datasets, these models encode rich, common-sense knowledge that can be leveraged in downstream tasks to improve performance. However, while

¹Department of Computer Science, Stanford University, USA
²Department of Computer Science, Carnegie Mellon University, USA. Correspondence to: Caroline Choi <cchoi1@stanford.edu>, Yoonho Lee <yoonho@stanford.edu>.

Preprint.

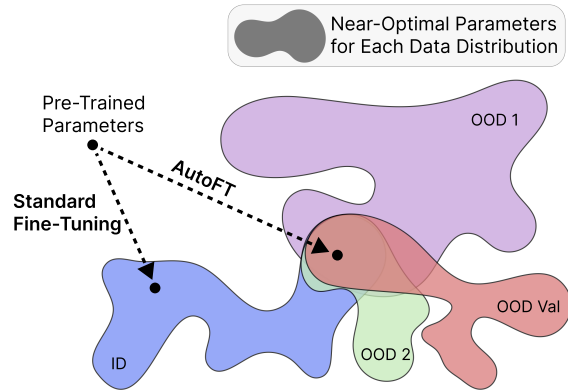


Figure 1: Overview of AUTOFT: a method for robustly fine-tuning foundation models. While fine-tuning with in-distribution (ID) data (blue), AUTOFT searches for a fine-tuning objective that maximizes performance on a small out-of-distribution validation set (red). This validation set serves as a proxy for performance on different distributions (green and purple), allowing AUTOFT to learn a robust fine-tuning procedure.

fine-tuning on additional task-specific data improves performance on the target distribution, it degrades performance on different distributions.

This issue has driven recent research on *robust* fine-tuning, which aims to produce an adapted model that achieves good performance under distribution shifts. Prior works have proposed various regularization techniques to preserve the prior knowledge embedded in the foundation model, such as ensembling models before and after adaptation (Wortsman et al., 2022b) or initially fitting only the last layer (Kumar et al., 2022a). However, these approaches propose hard-coded fine-tuning procedures, which may not fully capture the intricate relationship between foundation model priors and task-specific data during adaptation. Furthermore, this relationship can vary across fine-tuning tasks, and a one-size-fits-all approach may not account for these differences.

We introduce AUTOFT, a novel approach for robust fine-tuning that aims to optimally balance between preserving foundation model priors and incorporating task-specific knowledge during adaptation. Our key insight is that we can *learn* the best adaptation strategy for a given fine-tuning task. AUTOFT learns a fine-tuning objective and hyperparameters using a small out-of-distribution (OOD) validation set to produce models that are robust to distribution shifts.

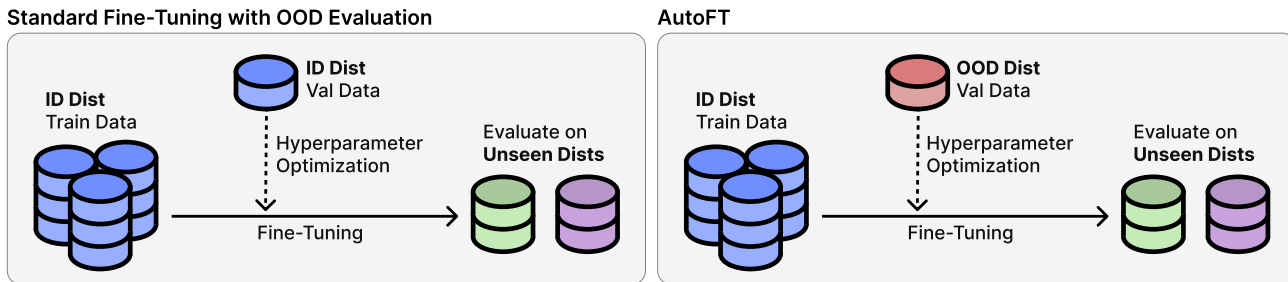


Figure 2: A summary of our data assumptions and evaluation protocol. The standard approach is to optimize hyperparameters on a validation dataset drawn from the same distribution as the training data. In contrast, AutoFT employs a small out-of-distribution (OOD) validation set for hyperparameter optimization, enhancing the generalizability of the final model. We evaluate all fine-tuned models on data from unseen distribution shifts (green and purple).

We then fine-tune the foundation model with the learned objective and hyperparameters and evaluate its robustness to new distribution shifts.

Our contributions are twofold. First, we learn the fine-tuning objective itself, parameterized by weight coefficients for several different loss functions and regularizers. This large search space gives AUTOFT more granular control over adaptation. Second, AUTOFT optimizes the fine-tuning objective and hyperparameters with respect to post-adaptation performance on a proxy distribution shift: an OOD validation set. Importantly, this validation set is drawn from a different distribution than the final evaluation datasets and is small, containing fewer than 1% of the number of examples in the fine-tuning dataset. We illustrate the intuition behind our approach in Figure 1 and our data assumptions in Figure 2.

We rigorously evaluate AUTOFT on a wide array of real-world datasets and consider various types of distribution shifts, including subpopulation and domain shift. Our experiments show that a model fine-tuned with the objective learned by AUTOFT generalizes better to previously unseen distribution shifts. With as few as 1000 examples from a different distribution than that of the fine-tuning data, which is often readily available, AUTOFT outperforms existing robust fine-tuning methods across all benchmarks. These gains in robustness are achieved with minimal additional compute, requiring at most 5% more compute compared to standard fine-tuning. Among other results, AUTOFT achieves new state-of-the-art performance on the challenging iWildCam and FMoW benchmarks (Beery et al., 2021; Koh et al., 2021; Christie et al., 2018), outperforming the prior best methods by 6.0% and 1.5%, respectively.

2 Related Work

Transfer learning. While early research demonstrated that using features learned from pre-training on large datasets are effective for new tasks, transfer learning has evolved to optimize performance in settings with limited data (Oquab et al., 2014; Yosinski et al., 2014; Sharif Razavian et al.,

2014). Common transfer learning techniques include fine-tuning with regularization (Zhang et al., 2020; Xuhong et al., 2018; Lee et al., 2019a; Jiang et al., 2019; Li et al., 2020; Aghajanyan et al., 2020; Gouk et al., 2021; Shen et al., 2021; Karani et al., 2021) and selectively freezing pre-trained parameters (Kirkpatrick et al., 2017; Lee et al., 2019b; Guo et al., 2019; Ramasesh et al., 2020; Liu et al., 2021b; Royer & Lampert, 2020; Eastwood et al., 2021; Evci et al., 2022; Eastwood et al., 2022; Cohen et al., 2022; Touvron et al., 2022; Lee et al., 2022a; Kumar et al., 2022b). However, as pre-trained models are fine-tuned for a specific distribution, their effective robustness decreases at convergence (Andreassen et al., 2021). We introduce a transfer learning framework that preserves the robustness of the pre-trained model while adapting to new tasks.

AutoML and bi-level optimization. Our work leverages high-level ideas from the broader literature on meta-learning and hyperparameter optimization. Such methods have proposed to optimize different parts of the training pipeline, including general hyperparameters (Hutter et al., 2011; Bergstra & Bengio, 2012; Feurer et al., 2015; Li et al., 2017; 2018b), network architectures (Zoph & Le, 2016; Zoph et al., 2018; Liu et al., 2018; Real et al., 2019; Xu et al., 2019), augmentation policies (Cubuk et al., 2019; Lim et al., 2019; Hataya et al., 2020; Cubuk et al., 2020), optimizers (Bengio et al., 2013; Andrychowicz et al., 2016; Wichrowska et al., 2017; Metz et al., 2022; Chen et al., 2023), and objective functions (Yu et al., 2018; Kirsch et al., 2019; Oh et al., 2020; Bechtle et al., 2021). However, most of these works optimize for generalization within the training distribution and do not consider robustness to distribution shifts. Existing works that optimize a training procedure for OOD generalization consider a structured few-shot adaptation setting (Li et al., 2018a; Zhang et al., 2021), limiting their scalability to large datasets. Tian et al. (2023) learn layer-specific regularization constraints to improve OOD generalization; however, they do not learn a fine-tuning objective.

Out-of-distribution generalization. Maintaining good per-

performance on data that deviates from the training distribution is crucial in many real-world applications, where models may face data from unfamiliar environments (Hendrycks & Dietterich, 2019; Geirhos et al., 2020; Gulrajani & Lopez-Paz, 2020; Koh et al., 2021). Numerous studies have investigated how to ensure robustness to various distribution shifts (Tzeng et al., 2014; Byrd & Lipton, 2019; Hendrycks et al., 2019; Arjovsky et al., 2019; Salman et al., 2020; Liu et al., 2021a; Wiles et al., 2021; Andreassen et al., 2021; Creager et al., 2021; Lee et al., 2022b). Some works have shown that despite the myriad of ways in which data distributions can change, naturally occurring distribution shifts have a surprisingly predictable effect on model performance (Taori et al., 2020; Miller et al., 2021; Baek et al., 2022), suggesting that it may be possible to *learn* how to be robust to unseen natural distribution shifts. Similar to our work, Goyal et al. (2022b) meta-learn an objective, but for test-time adaptation instead of fine-tuning. Benchmarks for OOD generalization, such as DomainBed (Gulrajani & Lopez-Paz, 2020) and WILDS (Koh et al., 2021), have discussed data assumptions for dealing with distribution shifts, and suggested that an OOD validation set can be a useful signal for hyperparameter optimization and model selection. AUTOFT leverages this signal much more directly than existing works by learning an objective for fine-tuning.

Robust fine-tuning. Foundation models trained on massive datasets encode a broad range of general knowledge, enabling robust performance across various data distributions, including OOD scenarios (Radford et al., 2021b; Bommasani et al., 2021). While in principle, foundation models should serve as a useful prior for further fine-tuning, empirical evidence shows that fine-tuning foundation models on a new task often leads to a significant drop in OOD performance (Andreassen et al., 2021). Recent works have proposed modifications to the basic fine-tuning procedure to improve OOD generalization (Wortsman et al., 2022b; Kumar et al., 2022a; Wortsman et al., 2022a; Goyal et al., 2022a; Mukhoti et al., 2023). Instead of hand-designing a regularization technique, we propose a data-driven approach to *learn* a more nuanced fine-tuning procedure. In fact, some prior works (Xuhong et al., 2018; Lee et al., 2022a; Goyal et al., 2022a) can be seen as *special cases* of AUTOFT since our hyperparameter search space encompasses these fine-tuning algorithms. Our experiments in Section 6 demonstrate that AUTOFT consistently outperforms prior robust fine-tuning methods on OOD data.

3 Background: Hyperparameter Optimization

We first formalize hyperparameter optimization as a means for searching the space of fine-tuning procedures in Section 4. Hyperparameters are predefined properties of the learning algorithm which are not learned during training,

such as network architecture, learning rate, and regularization strength. A good choice of hyperparameters can significantly improve model performance, yet optimal hyperparameters vary, depending on the data distribution and evaluation metrics.

Formally, we denote the learning algorithm as LearnAlg and its hyperparameters as $\phi \in \Phi$, where Φ is the hyperparameter space. We denote the training and validation datasets as D_{tr} and D_{val} , respectively. These datasets are disjoint and typically drawn from the same distribution. The learning algorithm LearnAlg produces a model by training on D_{tr} with hyperparameters ϕ . We denote the resulting model as LearnAlg(ϕ, D_{tr}). Hyperparameter optimization finds hyperparameters that maximize some performance metric Perf(f, D_{val}) which depends on the model f and the validation dataset D_{val} . Examples of performance metrics include top-1 accuracy, macro F1 score, and worst-region accuracy. We formalize hyperparameter optimization as

$$\phi^* = \arg \max_{\phi \in \Phi} \mathbb{E} \left[\overbrace{\text{Perf}(\text{LearnAlg}(\phi, D_{\text{tr}}), D_{\text{val}})}^{\text{Validation Set Performance}} \right]. \quad (1)$$

Learned Parameters

Here, the expectation is taken over any randomness in the learning algorithm LearnAlg, such as input data shuffling or random initialization. The optimized hyperparameters ϕ^* are subsequently used to train the model.

Hyperparameter optimization methods typically start with randomly initialized model parameters and use a validation set D_{val} , drawn from the same distribution as the training data, to adjust hyperparameters. The problem of robust fine-tuning, however, begins with pre-trained model parameters and aims to achieve high performance on test data that diverges from the fine-tuning distribution. In the next section, we describe how we leverage hyperparameter optimization to learn a robust adaptation procedure.

4 AUTOFT: Robust Fine-Tuning with a Learned Objective

In this section, we present AUTOFT, a data-driven approach for robust fine-tuning. Given a foundation model and task-specific data, AUTOFT uses bi-level optimization to learn a fine-tuning objective and optimal hyperparameters. There are two key components in AUTOFT. First, learning the fine-tuning objective enables a more precise adaptation to task-specific data. Second, AUTOFT optimizes the objective and hyperparameters for performance under a proxy distribution shift, which enhances OOD generalization.

4.1 Problem Setting: Robust Fine-Tuning

Data assumptions. We assume access to two datasets: (1) a large fine-tuning dataset D_{tr} from the training distribution \mathcal{P}_{tr} , and (2) a small held-out OOD validation set D_{val} from

Algorithm 1 AUTOFT

Require: Hyperparameter Optimizer (HPO)
Require: ID Training Data D_{tr} , OOD Validation Data D_{val}
 1: **for** $\phi \leftarrow \text{HPO.Sample}()$ **do**
 2: $f_{ft} \leftarrow \text{LearnAlg}(D_{\text{tr}}, \mathcal{L}_{\phi})$ // Short fine-tuning run
 with sampled loss
 3: $p \leftarrow \text{Perf}(f_{ft}, D_{\text{val}})$ // Evaluation on OOD Val set
 4: **end for**
 5: $\phi^* \leftarrow \text{HPO.Best}()$ // Get best hyperparameters
 6: $f^* \leftarrow \text{LearnAlg}(D_{\text{tr}}, \mathcal{L}_{\phi^*})$ // Fine-tune with loss \mathcal{L}_{ϕ^*}
 7: **Return** f^*

a different distribution \mathcal{P}_{val} . The validation set D_{val} is much smaller than D_{tr} , containing as few as 1000 examples, and is only used for outer-level optimization, not for fine-tuning. We then fine-tune on D_{tr} with the found hyperparameters and test the fine-tuned model on several OOD distributions $\mathcal{P}_{\text{ood}}^1, \mathcal{P}_{\text{ood}}^2, \dots$. Note that these test distributions are distinct from both \mathcal{P}_{tr} and \mathcal{P}_{val} , and are never shown to the model before final evaluation. Following prior works on robust fine-tuning, all distributions are assumed to be related to the same task. We consider domain and subpopulation shifts arising from differences in data collection. For instance, in animal recognition from camera trap images, each distribution may represent different locations (Beery et al., 2021; Koh et al., 2021). Such data is often readily available, as shown in the WILDS and DomainBed benchmarks (Koh et al., 2021; Gulrajani & Lopez-Paz, 2020), and can be constructed by partitioning by time or geographical location.

Notation and concrete setup. Let f denote a pre-trained foundation model with parameters θ , which we adapt by fine-tuning on D_{tr} . We denote the fine-tuning algorithm as $\text{LearnAlg}(\phi, D_{\text{tr}})$, where ϕ specifies both the fine-tuning objective and other hyperparameters such as learning rate. In our experiments, the performance metric Perf follows the standards in each evaluation setting and is either top-1 accuracy, worst-region accuracy, or macro F1.

4.2 Learning a Fine-Tuning Objective via Bi-Level Optimization

Formulation. We frame the problem of learning a fine-tuning objective as a bi-level optimization problem with the form (1), which we can solve using existing black-box hyperparameter optimizers. Practically, solving this bi-level optimization problem involves fine-tuning the same foundation model multiple times, each time with different “hyperparameters” ϕ^1, ϕ^2, \dots to obtain different final fine-tuned models $f^1 = \text{LearnAlg}(\phi^1, D_{\text{tr}}), f^2 = \dots$. We then evaluate the quality of each ϕ^i through the performance of f^i on the OOD validation set; by aggregating the information from these different fine-tuning runs, we can fine good hyperpa-

rameters ϕ^* . At test time, we fine-tune the initial foundation model with ϕ^* and evaluate its performance on novel OOD distributions to assess its generalization capabilities. We summarize this procedure in Algorithm 1.

Parameterization of the fine-tuning objective. The main novelty of AUTOFT is that we parameterize the fine-tuning objective, which allows outer-loop optimization to search over an expressive space of fine-tuning algorithms. This extra expressivity is important: for robust fine-tuning, the algorithm must selectively *ignore* some aspects of the training distribution in order to better generalize to novel OOD distributions. Specifically, we allow Φ to express the fine-tuning objective by learning weights for a pre-defined set of loss functions and regularizers. Note that the cross-entropy and hinge losses similarly guide the model’s predictions towards the correct label, but with a different amount of penalty for severely incorrect samples. As another example, the contrastive loss on image-text pairs (Radford et al., 2021b; Goyal et al., 2022a) also guides the model’s predictions towards the correct label, but in a way that incorporates language embeddings, which is entirely different from how the cross-entropy and hinge losses operate.

Therefore, we consider weight coefficients for nine different loss functions and regularizers: cross-entropy loss, hinge loss, image-text contrastive loss, entropy, confidence minimization, L1 norm, L2 norm, L1 and L2 distance to pre-trained model parameters. We select these losses to address various aspects of model learning and generalization, such as classification accuracy, decision confidence, and prevention of overfitting, ensuring a nuanced and effective model adaptation. We denote these loss weight coefficients as $W = \{w_1, w_2, \dots, w_9\}$. Denoting the i -th loss function or regularizer as \mathcal{L}_i , the total loss \mathcal{L} is the weighted sum $\mathcal{L} = \sum_{i=1}^9 w_i \mathcal{L}_i$. To enable finer control over the speed and stability of adaptation during fine-tuning, we additionally learn hyperparameters for the fine-tuning optimizer: learning rate η , weight decay δ , and random seed σ . Our complete set of hyperparameters for outer-loop optimization is thus $\phi = (W, \eta, \delta, \sigma)$.

Bi-level optimization algorithm. We need a black-box optimizer that can effectively search through the high-dimensional hyperparameter space Φ . We use the Tree-structured Parzen Estimator (Bergstra et al., 2011, TPE) for this purpose, as its design allows for efficient processing in high-dimensional spaces and yields effective results at the order of hundreds of evaluations. TPE creates a probabilistic model from previous hyperparameter evaluations, and differentiates between better and worse hyperparameter configurations by comparing their likelihood under two separate models. We use the TPE implementation from the `optuna` library (Akiba et al., 2019). Experiments in Table 8 demonstrate that in the context of learning a fine-tuning objective,

TPE outperforms other bi-level optimizers such as random search, quasi Monte Carlo, and Bayesian optimization.

As the prior distribution for TPE, we use an appropriately scaled distribution for each hyperparameter, operating in log-space for the weight coefficients and learning rate since the optimal values can vary over several orders of magnitude:

$$w_i \sim \text{LogUniform}(w_{\min}, w_{\max}), \quad \rho \sim [0, 100]$$

$$\eta \sim \text{LogUniform}(\eta_{\min}, \eta_{\max}), \quad \delta \sim \text{Uniform}(0.0, 1.0).$$

We find that in practice, $(w_{\min}, w_{\max}) = (10^{-4}, 10)$ is an effective range for all w_i . Given a model’s conventional learning rate η^* , we set $(\eta_{\min}, \eta_{\max}) = (10^{-2}\eta^*, 10^2\eta^*)$.

Intuition for OOD evaluation. Optimizing the objective with respect to performance on a small out-of-distribution (OOD) validation set D_{val} can guide the model to learn more generalizable parameters during fine-tuning. We conduct a didactic toy experiment in Appendix A, which illustrates our key intuition: a small validation set reveals *how* the data distribution changes under natural shifts, informing how best to adapt a given foundation model. Our experiments in Section 6 confirm that AUTOFT consistently improves generalization to novel OOD distributions, outperforming state-of-the-art methods.

Computational cost. The bi-level optimization of AUTOFT introduces minimal computational overhead, requiring at most 5% additional compute compared to one standard fine-tuning run on most benchmarks. Each evaluation of the objective and hyperparameters requires a small number of inner loop gradient steps on the fine-tuning dataset. AUTOFT is therefore computationally inexpensive, and highly practical for even large fine-tuning problem settings. Hyperparameters are detailed in Appendix D.4.

5 Experimental Setup

Evaluation. We fine-tune pre-trained CLIP models from the `open-clip` repository (Radford et al., 2021b; Ilharco et al., 2021). We use the CLIP ViT-B/16 model from OpenAI as our default model, unless specified otherwise. Our SoTA results on WILDS-iWildCam and WILDS-FMoW use the CLIP ViT-L/14-336px model. We use text templates used in prior work (Radford et al., 2021b; Wortsman et al., 2022b) to generate zero-shot classification weights.

Following prior works on robust fine-tuning, we evaluate AUTOFT on nine *natural distribution shifts*, few-shot learning, and transfer learning settings (Taori et al., 2020; Radford et al., 2021b; Wortsman et al., 2022b; Kumar et al., 2022a; Goyal et al., 2022a). These include five ImageNet distribution shifts (IN-V2, IN-R, IN-Sketch, ObjectNet, and IN-A) (Recht et al., 2019; Hendrycks et al., 2021a; Wang et al., 2019; Barbu et al., 2019; Hendrycks et al., 2021b), WILDS-iWildCam (Koh et al., 2021; Beery et al., 2021),

WILDS-FMoW (Koh et al., 2021; Christie et al., 2018), CIFAR-10.1 (Recht et al., 2018; Torralba et al., 2008), and CIFAR-10.2 (Lu et al., 2020). We use up to 1000 examples from ImageNet-C, OOD validation splits of WILDS-FMoW and WILDS-iWildCam, and CIFAR-10-C as the OOD validation sets. We also evaluate on few-shot classification (Figure 4 and Figure 7) and transfer learning (Table 10).

Effective robustness and weight ensembling curves. We primarily evaluate robustness to distribution shifts using average OOD performance. We also compare methods with weight ensembling of the zero-shot and fine-tuned models (Wortsman et al., 2022b), which enhances ID and OOD performance in a way orthogonal to fine-tuning. We interpolate model weights with ten mixing coefficients, α , and report results using the coefficient that maximizes ID validation accuracy. Finally, we plot ID and OOD performance across these different interpolation coefficients in Figure 3 to visualize *effective robustness* – gains in accuracy beyond the zero-shot model, which corresponds to *vertical distance* between curves.

Baselines. We compare AUTOFT against several methods for adapting pretrained models. We include two standard transfer learning methods that minimize cross-entropy loss: linear probing (LP) and full fine-tuning (FT). We also compare with recent works in robust fine-tuning: L2-SP (Li et al., 2018b), which fine-tunes with an L2 regularization term towards pretrained weights; LP-FT (Kumar et al., 2022a), which performs linear probing followed by full fine-tuning; Freeze-Embed (Kumar et al., 2022b), which freezes the embedding layer during fine-tuning; and FLYP (Goyal et al., 2022a), which fine-tunes with the CLIP pretraining loss – a contrastive loss between image embeddings and class-descriptive prompt embeddings. As we are interested in OOD performance, we also compare against OOD generalization methods, including Group DRO (Sagawa et al., 2019), ABSGD (Qi et al., 2020), LISA (Yao et al., 2022), DFR (Kirichenko et al., 2022), and Copy-Paste (Gao et al., 2023). We additionally evaluate all methods with weight ensembling (WiSE-FT) (Wortsman et al., 2022b), which is shown to improve OOD performance in an orthogonal way to other robust fine-tuning methods.

Bi-level optimization details. We summarize the number

| Dataset | Steps | Trials | N_{val} |
|----------|-------|--------|------------------|
| iWildCam | 10 | 500 | 1000 |
| FMoW | 10 | 500 | 1000 |
| CIFAR-10 | 10 | 100 | 100 |
| Flowers | 50 | 500 | 500 |
| Cars | 50 | 500 | 1000 |
| ImageNet | 100 | 500 | 1000 |

Table 1: AUTOFT training settings for each dataset.

| Method | Architecture | ID | OOD |
|---------------|--------------|------------|-------------------|
| Group DRO | ResNet50 | 37.5 (1.9) | 23.8 (2.0) |
| ABSGD | ResNet50 | 47.5 (1.6) | 33.0 (0.6) |
| Copy-Paste | ResNet50 | 50.2 (1.6) | 36.5 (0.9) |
| ERM | PNASNet | 52.8 (1.4) | 38.5 (0.6) |
| ERM | ViTL | 55.8 (1.9) | 41.4 (0.5) |
| Model Soups | ViTL | 57.6 (1.9) | 43.3 (1.0) |
| FLYP | ViTL-336px | 59.9 (0.7) | 46.0 (1.3) |
| AUTOFT | ViTL-336px | 63.5 (0.5) | 52.0 (0.4) |

Table 2: **iWildCam SoTA results.** AUTOFT with weight ensembling attains state-of-the-art OOD performance on the WILDS-iWildCam benchmark with a ViT-L/14-336px backbone, surpassing all prior entries on the WILDS leaderboard (Koh et al., 2021).

| Method | Architecture | ID | OOD |
|---------------|--------------|------------|-------------------|
| Group DRO | DenseNet121 | 51.2 (0.4) | 31.1 (1.7) |
| LISA | DenseNet121 | 52.8 (1.2) | 35.5 (0.8) |
| ERM w/ aug | DenseNet121 | 55.5 (0.4) | 35.7 (0.3) |
| DFR | DenseNet121 | 53.4 (0.4) | 42.8 (0.4) |
| ERM | ViTL | 66.9 (0.2) | 46.1 (0.6) |
| Model Soups | ViTL | 69.5 (0.1) | 47.6 (0.3) |
| Freeze-Embed | ViTL-336px | 68.3 (0.4) | 50.3 (1.1) |
| AUTOFT | ViTL-336px | 72.1 (0.1) | 51.8 (0.4) |

Table 3: **FMoW SoTA results.** AUTOFT with weight ensembling attains state-of-the-art OOD performance on the WILDS-FMoW benchmark with a ViT-L/14-336px backbone, surpassing all prior entries on the WILDS leaderboard (Koh et al., 2021).

of inner-loop gradient steps, outer-loop fine-tuning trials, and validation set size for each dataset in Table 1. All of these values were selected based on performance on an ID validation set. We provide additional details on our training protocol in Appendix D.4.

6 Results

In this section, we present the main experimental findings for AUTOFT. We show that AUTOFT improves OOD generalization on nine distribution shifts. We present additional results in the low-data and IID transfer learning regimes in Section 6.2 and Section 6.3. These findings highlight the effectiveness of AUTOFT for robust fine-tuning in a variety of settings. Finally, we investigate several aspects of the AUTOFT method, including transferability of the learned objective across datasets, the choice of validation dataset and hyperparameter optimization algorithm. Further experimental details are in Appendix D.

6.1 Distribution Shifts

Improvements in OOD generalization. We evaluate AUTOFT on three common robust fine-tuning benchmarks: Ima-

geNet, WILDS-FMoW, and WILDS-iWildCam. This evaluation includes diverse distribution shift conditions including subpopulation and domain shifts. ID and OOD performance reported in Table 4 show that AUTOFT consistently outperforms existing methods for robust fine-tuning in OOD metrics. Furthermore, these gains are maintained when ensembling initial and fine-tuned models, suggesting that the benefits from AUTOFT are complementary to that of ensembling (Wortsman et al., 2022b;a). We show additional experiments on CIFAR-10 and related distribution shifts in Table 11, which show the same conclusion.

State-of-the-art performance on iWildCam and FMoW.

To further assess whether the robustness gains from AUTOFT scale to larger foundation models, we evaluate AUTOFT with a ViT-L/14@336px model, following the largest scale experiment in Goyal et al. (2022a). Results in Table 2 show that AUTOFT improves upon the prior state-of-the-art method, FLYP (Goyal et al., 2022a), by 6.0% in OOD macro-F1. Furthermore, on WILDS-FMoW Table 3, AUTOFT outperforms a Transformer-specific parameter freezing method (Kumar et al., 2022b), the prior state-of-the-art, by 1.5% in OOD worst-region accuracy. Additionally, AUTOFT outperforms the compute-intensive Model Soups (Wortsman et al., 2022a) on both benchmarks; this method ensembles more than 70 models fine-tuned with different augmentations and hyperparameters.

6.2 Few-Shot Classification

Few-shot classification serves as an important benchmark in applications where there are small quantities of labeled data available for fine-tuning. Few-shot binary classification is particularly challenging, given the small number of training examples. We evaluate on 4, 16, and 32 shot binary classification tasks from the PatchCamelyon and Rendered-SST2 datasets, following Radford et al. (2021b) and Goyal et al. (2022a). PatchCamelyon contains digital pathology images for the detection of metastatic tissue. Rendered-SST2 focuses on optical character recognition for classifying text sentiment.

Figure 4 shows that AUTOFT still improves effective robustness with limited data, outperforming FLYP by 3.7% and full fine-tuning by 3.9% in a challenging 4-shot classification task on Rendered-SST2.

6.3 Transfer Learning

We additionally evaluate AUTOFT on standard transfer learning tasks, where the evaluation data is drawn from the same distribution as both the training and validation data. We compare AUTOFT against other fine-tuning methods on several transfer learning datasets: CalTech-101, Stanford Cars, and Flowers-102. Results in Table 10 demonstrate that AUTOFT is competitive with these baselines, but the advan-

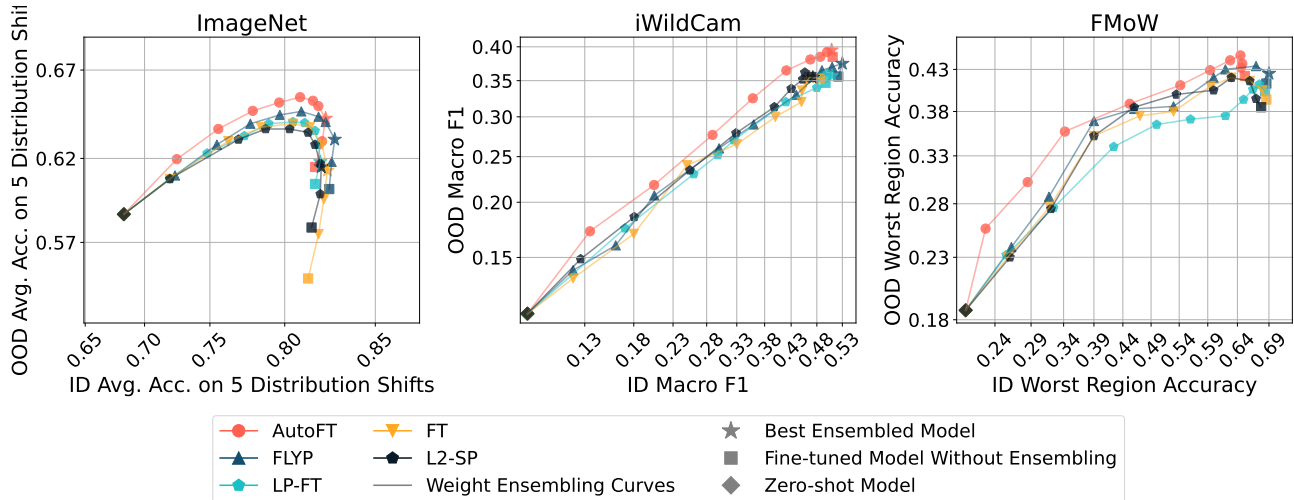


Figure 3: AUTOFT outperforms existing methods, both with and without weight ensembling (Wortsman et al., 2022b). Here, we show the ID-OOD performance curves obtained by linearly interpolating weights of the fine-tuned model weights with the zero-shot model.

| Methods | ImageNet | | | | iWILDCam | | | | FMoW | |
|----------|--------------------|-------------------|-----------------|-------------------|--------------------|-------------------|-----------------|-------------------|--------------------|-------------------|
| | Without Ensembling | | With Ensembling | | Without Ensembling | | With Ensembling | | Without Ensembling | |
| | ID | OOD | ID | OOD | ID | OOD | ID | OOD | ID | OOD |
| Zeroshot | 68.3 (-) | 58.7 (-) | 68.3 (-) | 58.7 (-) | 8.7 (-) | 11.0 (-) | 8.7 (-) | 11.0 (-) | 20.4 (-) | 18.7 (-) |
| LP | 79.9 (0.0) | 57.2 (0.0) | 80.0 (0.0) | 58.3 (0.0) | 44.5 (0.6) | 31.1 (0.4) | 45.5 (0.6) | 31.7 (0.4) | 48.2 (0.1) | 30.5 (0.3) |
| FT | 81.4 (0.1) | 54.8 (0.1) | 82.5 (0.1) | 61.3 (0.1) | 48.1 (0.5) | 35.0 (0.5) | 48.1 (0.5) | 35.0 (0.5) | 68.5 (0.1) | 39.2 (0.7) |
| L2-SP | 81.6 (0.1) | 57.9 (0.1) | 82.2 (0.1) | 58.9 (0.1) | 48.6 (0.4) | 35.3 (0.3) | 48.6 (0.4) | 35.3 (0.3) | 68.6 (0.1) | 39.4 (0.6) |
| LP-FT | 81.8 (0.1) | 60.5 (0.1) | 82.1 (0.1) | 61.8 (0.1) | 49.7 (0.5) | 34.7 (0.4) | 50.2 (0.5) | 35.7 (0.4) | 68.4 (0.2) | 40.4 (1.0) |
| FLYP | 82.6 (0.0) | 60.2 (0.1) | 82.9 (0.0) | 63.2 (0.1) | 52.2 (0.6) | 35.6 (1.2) | 52.5 (0.6) | 37.1 (1.2) | 68.6 (0.2) | 41.3 (0.8) |
| AUTOFT | 81.8 (0.1) | 61.5 (0.1) | 82.4 (0.1) | 64.3 (0.1) | 51.0 (0.5) | 38.3 (0.5) | 51.3 (0.5) | 39.3 (0.5) | 67.1 (0.3) | 42.3 (0.5) |

Table 4: AUTOFT outperforms all baselines, both with and without ensembling. Without ensembling, AUTOFT improves OOD performance by 1.3% on ImageNet, 2.7% on WILDS-iWildCam, and 1.0% on WILDS-FMoW. These improvements are preserved with weight ensembling.

| Method | ID | OOD |
|-------------------------------|-------------|-------------|
| FT | 48.1 | 35.0 |
| AUTOFT, transferred objective | 49.9 | 35.5 |
| AUTOFT | 51.0 | 38.3 |

Table 5: Learning a fine-tuning objective on the task of interest (AUTOFT) outperforms fine-tuning with an objective learned on a different task (AUTOFT, transferred objective). This suggests that the learned objective is not universal, but specific to the task on which it is optimized.

tages from learning an objective are less pronounced compared to previous experiments. This suggests that problem-specific learned fine-tuning objectives are most helpful in settings with high underspecification, such as OOD evaluation conditions or few-shot learning, confirming our initial intuition in Section 4.

| Method | Validation Set | OOD Test |
|--------|----------------|-------------------|
| FT | CIFAR-10 | 93.6 (0.2) |
| AUTOFT | CIFAR-10 | 95.1 (0.2) |
| | CIFAR-10-C | 95.5 (0.2) |
| | CINIC | 94.5 (0.2) |
| | CIFAR-10.1 | 94.8 (0.3) |
| | CIFAR-10.2 | 95.3 (0.3) |

Table 6: AUTOFT outperforms fine-tuning with several different validation sets. We fine-tune on CIFAR-10 and use 100 examples from either the ID distribution (CIFAR-10) or a non-ID distribution (CIFAR-10-C, CINIC, CIFAR-10.1, CIFAR-10.2) to learn the objective and hyperparameters. Evaluation is on held-out examples from CIFAR-10.1 and CIFAR-10.2.

6.4 Analysis

Transferability of the learned objective. We evaluate models fine-tuned on WILDS-iWildCam with an objective

| k (shots) | PatchCamelyon | | | SST2 | | | Examples | ID | OOD |
|---------------|-------------------|-------------------|-------------------|-------------------|-------------------|-------------------|----------|-------------|-------------|
| | 4 | 16 | 32 | 4 | 16 | 32 | | | |
| Zeroshot | 56.5 (-) | 56.5 (-) | 56.5 (-) | 60.5 (-) | 60.5 (-) | 60.5 (-) | 200 | 48.9 | 37.2 |
| LP | 60.4 (4.0) | 64.4 (3.7) | 67.0 (4.4) | 60.8 (1.8) | 61.9 (1.4) | 62.9 (1.3) | 1000 | 51.0 | 38.3 |
| FT | 63.1 (5.5) | 71.6 (4.6) | 75.2 (3.7) | 61.1 (0.7) | 62.4 (1.6) | 63.4 (1.9) | 5000 | 50.4 | 38.0 |
| LP-FT | 62.7 (5.3) | 69.8 (5.3) | 73.9 (4.6) | 60.9 (2.4) | 62.9 (1.9) | 63.6 (1.4) | 10000 | 48.9 | 37.8 |
| FLYP | 66.9 (5.0) | 74.5 (2.0) | 76.4 (2.4) | 61.3 (2.7) | 65.6 (2.1) | 68.0 (1.7) | | | |
| AUTOFT | 68.1 (5.1) | 76.8 (2.9) | 79.5 (2.0) | 65.0 (3.8) | 67.5 (1.1) | 69.0 (1.1) | | | |

Figure 4: In binary few-shot classification, AUTOFT outperforms existing robust fine-tuning methods. AUTOFT outperforms FLYP by 3.1% and full fine-tuning by 4.3% in 32-shot classification on PatchCamelyon.

Figure 5: Test performance of AUTOFT on WILDS-iWildCam with varying validation set sizes. Increasing size beyond 1000 shows minimal additional benefits.

| Validation Set | ID Test | OOD Test |
|----------------|-------------|-------------|
| ID Validation | 52.3 | 35.8 |
| OOD Validation | 51.0 | 38.3 |

Table 7: Using a non-ID validation set improves OOD generalization compared to using an ID validation set. We evaluate AUTOFT on WILDS-iWildCam, using either the ID or OOD validation split from the WILDS benchmark to learn the objective and hyperparameters. Using an ID validation set improves ID performance, while using a non-ID validation set improves OOD performance.

| Hyperparameter Optimization | ID Test | OOD Test |
|----------------------------------|-------------|-------------|
| Random | 29.8 | 24.5 |
| Quasi Monte Carlo | 48.2 | 34.7 |
| Bayesian Optimization | 49.9 | 36.5 |
| Tree-Structured Parzen Estimator | 51.0 | 38.3 |

Table 8: We run AUTOFT with various hyperparameter optimization algorithms given the same computational budget. Evaluation is on WILDS-iWildCam. The Tree-Structured Parzen Estimator (TPE) outperforms other methods by a large margin.

learned on the same WILDS-iWildCam task (AUTOFT) or a different task, WILDS-FMoW (AUTOFT, transferred objective). We additionally compare with standard fine-tuning (FT) in Table 5. Fine-tuning with an objective learned on a different task (AUTOFT, transferred objective) degrades performance, suggesting that the learned objective is not universal, but tailored to the task on which it is optimized.

Choice of dataset for evaluating the learned hyperparameters. In Table 7, we run AUTOFT with different validation sets – the official ID validation, OOD validation, and OOD test splits from the WILDS-iWildCam benchmark. Optimizing hyperparameters with respect to an ID validation set improves ID performance, while using a non-ID validation set improves OOD generalization.

Choice of hyperparameter optimization algorithm. We assess the effect of different hyperparameter optimization al-

gorithms on the performance of AUTOFT. We run AUTOFT with three different hyperparameter optimization methods: random search, quasi Monte Carlo, and Bayesian optimization. Results in Table 8 show that Tree-Structured Parzen Estimator (TPE) outperforms other hyperparameter optimization methods.

Effect of validation set size. We examine the effect of validation set size on performance in Figure 5. Across all validation set sizes, AUTOFT yields improvements in OOD performance compared to the leading fine-tuning baseline (FLYP: 35.6%). Given a fixed number of inner steps and hyperparameter evaluations, there’s an optimal range for validation set size, beyond which additional benefits are minimal.

7 Conclusion

We introduce AUTOFT, a novel, data-driven approach for robust fine-tuning that learns the objective and hyperparameters. With a small amount of data from one OOD distribution, which is often readily available, AUTOFT outperforms prior fine-tuning methods. Notably, AUTOFT attains state-of-the-art performance on two WILDS benchmarks.

Limitations. AUTOFT is a general recipe for robust adaptation, and our specific implementation is only one instantiation. We expect that future work can improve upon AUTOFT by investigating other loss parameterizations and meta-optimization techniques within the AUTOFT framework. While our experiments show strong results in image classification, we have not yet evaluated AUTOFT in other problem settings, such as natural language processing (NLP). We hope that our work will inspire future work on data-driven approaches for robust adaptation.

Acknowledgements

We thank Kyle Hsu, Lukas Haas, and members of the IRIS lab for helpful feedback and discussions. We also thank Sachin Goyal for help with ImageNet experiments. This work was supported by KFAAS and NSF. A.R. is supported by Schmidt Futures, Google, Apple, and Open Philanthropy. C.F. is supported by ONR grant N00014-21-1-2685 and the NSF CAREER award.

References

- Aghajanyan, A., Shrivastava, A., Gupta, A., Goyal, N., Zettlemoyer, L., and Gupta, S. Better fine-tuning by reducing representational collapse. *arXiv preprint arXiv:2008.03156*, 2020. 2
- Akiba, T., Sano, S., Yanase, T., Ohta, T., and Koyama, M. Optuna: A next-generation hyperparameter optimization framework. In *Proceedings of the 25th ACM SIGKDD international conference on knowledge discovery & data mining*, pp. 2623–2631, 2019. 4
- Andreassen, A., Bahri, Y., Neyshabur, B., and Roelofs, R. The evolution of out-of-distribution robustness throughout fine-tuning. *arXiv preprint arXiv:2106.15831*, 2021. 2, 3
- Andrychowicz, M., Denil, M., Gomez, S., Hoffman, M. W., Pfau, D., Schaul, T., Shillingford, B., and De Freitas, N. Learning to learn by gradient descent by gradient descent. *Advances in neural information processing systems*, 29, 2016. 2
- Arjovsky, M., Bottou, L., Gulrajani, I., and Lopez-Paz, D. Invariant risk minimization. *arXiv preprint arXiv:1907.02893*, 2019. 3
- Baek, C., Jiang, Y., Raghunathan, A., and Kolter, J. Z. Agreement-on-the-line: Predicting the performance of neural networks under distribution shift. *Advances in Neural Information Processing Systems*, 35:19274–19289, 2022. 3
- Barbu, A., Mayo, D., Alverio, J., Luo, W., Wang, C., Gutfreund, D., Tenenbaum, J., and Katz, B. Objectnet: A large-scale bias-controlled dataset for pushing the limits of object recognition models. *Advances in neural information processing systems*, 32, 2019. 5, 18
- Bechtle, S., Molchanov, A., Chebotar, Y., Grefenstette, E., Righetti, L., Sukhatme, G., and Meier, F. Meta learning via learned loss. In *2020 25th International Conference on Pattern Recognition (ICPR)*, pp. 4161–4168. IEEE, 2021. 2
- Beery, S., Agarwal, A., Cole, E., and Birodkar, V. The iwildcam 2021 competition dataset. *arXiv preprint arXiv:2105.03494*, 2021. 2, 4, 5, 18
- Bengio, S., Bengio, Y., Cloutier, J., and Gescei, J. On the optimization of a synaptic learning rule. In *Optimality in Biological and Artificial Networks?*, pp. 281–303. Routledge, 2013. 2
- Bergstra, J. and Bengio, Y. Random search for hyperparameter optimization. *Journal of machine learning research*, 13(2), 2012. 2
- Bergstra, J., Bardenet, R., Bengio, Y., and Kégl, B. Algorithms for hyper-parameter optimization. In Shawe-Taylor, J., Zemel, R., Bartlett, P., Pereira, F., and Weinberger, K. (eds.), *Advances in Neural Information Processing Systems*, volume 24. Curran Associates, Inc., 2011. 4
- Bommasani, R., Hudson, D. A., Adeli, E., Altman, R., Arora, S., von Arx, S., Bernstein, M. S., Bohg, J., Bosselut, A., Brunskill, E., et al. On the opportunities and risks of foundation models. *arXiv preprint arXiv:2108.07258*, 2021. 3
- Byrd, J. and Lipton, Z. What is the effect of importance weighting in deep learning? In *International Conference on Machine Learning*, pp. 872–881. PMLR, 2019. 3
- Chen, X., Liang, C., Huang, D., Real, E., Wang, K., Liu, Y., Pham, H., Dong, X., Luong, T., Hsieh, C.-J., et al. Symbolic discovery of optimization algorithms. *arXiv preprint arXiv:2302.06675*, 2023. 2
- Christie, G., Fendley, N., Wilson, J., and Mukherjee, R. Functional map of the world. In *Proceedings of the IEEE Conference on Computer Vision and Pattern Recognition*, pp. 6172–6180, 2018. 2, 5, 18
- Cohen, N., Gal, R., Meiri, E. A., Chechik, G., and Atzmon, Y. "this is my unicorn, fluffy": Personalizing frozen vision-language representations. *arXiv preprint arXiv:2204.01694*, 2022. 2
- Creager, E., Jacobsen, J.-H., and Zemel, R. Environment inference for invariant learning. In *International Conference on Machine Learning*, pp. 2189–2200. PMLR, 2021. 3
- Cubuk, E. D., Zoph, B., Mane, D., Vasudevan, V., and Le, Q. V. Autoaugment: Learning augmentation strategies from data. In *Proceedings of the IEEE/CVF conference on computer vision and pattern recognition*, pp. 113–123, 2019. 2
- Cubuk, E. D., Zoph, B., Shlens, J., and Le, Q. V. Randaugment: Practical automated data augmentation with a reduced search space. In *Proceedings of the IEEE/CVF conference on computer vision and pattern recognition workshops*, pp. 702–703, 2020. 2

- Deng, J., Dong, W., Socher, R., Li, L.-J., Li, K., and Fei-Fei, L. Imagenet: A large-scale hierarchical image database. In *2009 IEEE conference on computer vision and pattern recognition*, pp. 248–255. Ieee, 2009. 18
- Eastwood, C., Mason, I., Williams, C. K., and Schölkopf, B. Source-free adaptation to measurement shift via bottom-up feature restoration. *arXiv preprint arXiv:2107.05446*, 2021. 2
- Eastwood, C., Mason, I., and Williams, C. K. Unit-level surprise in neural networks. In *I (Still) Can't Believe It's Not Better! Workshop at NeurIPS 2021*, pp. 33–40. PMLR, 2022. 2
- Evcı, U., Dumoulin, V., Larochelle, H., and Mozer, M. C. Head2toe: Utilizing intermediate representations for better transfer learning. In *International Conference on Machine Learning*, pp. 6009–6033. PMLR, 2022. 2
- Fei-Fei, L., Fergus, R., and Perona, P. Learning generative visual models from few training examples: An incremental bayesian approach tested on 101 object categories. In *Computer Vision and Pattern Recognition Workshop*. IEEE, 2004. 18
- Feurer, M., Klein, A., Eggenberger, K., Springenberg, J., Blum, M., and Hutter, F. Efficient and robust automated machine learning. *Advances in neural information processing systems*, 28, 2015. 2
- Gao, I., Sagawa, S., Koh, P. W., Hashimoto, T., and Liang, P. Out-of-domain robustness via targeted augmentations. *arXiv preprint arXiv:2302.11861*, 2023. 5
- Geirhos, R., Jacobsen, J.-H., Michaelis, C., Zemel, R., Brendel, W., Bethge, M., and Wichmann, F. A. Shortcut learning in deep neural networks. *Nature Machine Intelligence*, 2(11):665–673, 2020. 3
- Gouk, H., Hospedales, T., and massimiliano pontil. Distance-based regularisation of deep networks for fine-tuning. In *International Conference on Learning Representations*, 2021. 2
- Goyal, S., Kumar, A., Garg, S., Kolter, Z., and Raghunathan, A. Finetune like you pretrain: Improved fine-tuning of zero-shot vision models. *arXiv preprint arXiv:2212.00638*, 2022a. 3, 4, 5, 6, 16, 17, 18
- Goyal, S., Sun, M., Raghunathan, A., and Kolter, J. Z. Test time adaptation via conjugate pseudo-labels. *Advances in Neural Information Processing Systems*, 35:6204–6218, 2022b. 3
- Gulrajani, I. and Lopez-Paz, D. In search of lost domain generalization. *arXiv preprint arXiv:2007.01434*, 2020. 3, 4
- Guo, Y., Shi, H., Kumar, A., Grauman, K., Rosing, T., and Feris, R. Spottune: transfer learning through adaptive fine-tuning. In *Proceedings of the IEEE/CVF conference on computer vision and pattern recognition*, pp. 4805–4814, 2019. 2
- Hataya, R., Zdenek, J., Yoshizoe, K., and Nakayama, H. Faster autoaugment: Learning augmentation strategies using backpropagation. In *Computer Vision—ECCV 2020: 16th European Conference, Glasgow, UK, August 23–28, 2020, Proceedings, Part XXV 16*, pp. 1–16. Springer, 2020. 2
- Hendrycks, D. and Dietterich, T. Benchmarking neural network robustness to common corruptions and perturbations. *Proceedings of the International Conference on Learning Representations*, 2019. 3
- Hendrycks, D., Mazeika, M., Kadavath, S., and Song, D. Using self-supervised learning can improve model robustness and uncertainty. *Advances in neural information processing systems*, 32, 2019. 3
- Hendrycks, D., Basart, S., Mu, N., Kadavath, S., Wang, F., Dorundo, E., Desai, R., Zhu, T., Parajuli, S., Guo, M., et al. The many faces of robustness: A critical analysis of out-of-distribution generalization. In *Proceedings of the IEEE/CVF International Conference on Computer Vision*, pp. 8340–8349, 2021a. 5, 18
- Hendrycks, D., Zhao, K., Basart, S., Steinhardt, J., and Song, D. Natural adversarial examples. In *Proceedings of the IEEE/CVF Conference on Computer Vision and Pattern Recognition*, pp. 15262–15271, 2021b. 5, 18
- Hutter, F., Hoos, H. H., and Leyton-Brown, K. Sequential model-based optimization for general algorithm configuration. In *Learning and Intelligent Optimization: 5th International Conference, LION 5, Rome, Italy, January 17-21, 2011. Selected Papers 5*, pp. 507–523. Springer, 2011. 2
- Ilharcó, G., Wortsman, M., Wightman, R., Gordon, C., Carlini, N., Taori, R., Dave, A., Shankar, V., Namkoong, H., Miller, J., Hajishirzi, H., Farhadi, A., and Schmidt, L. Openclip. Zenodo, July 2021. doi: 10.5281/zenodo.5143773. If you use this software, please cite it as below. 1, 5
- Jia, C., Yang, Y., Xia, Y., Chen, Y.-T., Parekh, Z., Pham, H., Le, Q., Sung, Y.-H., Li, Z., and Duerig, T. Scaling up visual and vision-language representation learning with noisy text supervision. In *International conference on machine learning*, pp. 4904–4916. PMLR, 2021. 1
- Jiang, H., He, P., Chen, W., Liu, X., Gao, J., and Zhao, T. Smart: Robust and efficient fine-tuning for pre-trained

- natural language models through principled regularized optimization. *arXiv preprint arXiv:1911.03437*, 2019. 2
- Karani, N., Erdil, E., Chaitanya, K., and Konukoglu, E. Test-time adaptable neural networks for robust medical image segmentation. *Medical Image Analysis*, 68:101907, 2021. ISSN 1361-8415. 2
- Kirichenko, P., Izmailov, P., and Wilson, A. G. Last layer re-training is sufficient for robustness to spurious correlations. *arXiv preprint arXiv:2204.02937*, 2022. 5
- Kirkpatrick, J., Pascanu, R., Rabinowitz, N., Veness, J., Desjardins, G., Rusu, A. A., Milan, K., Quan, J., Ramalho, T., Grabska-Barwinska, A., et al. Overcoming catastrophic forgetting in neural networks. *Proceedings of the national academy of sciences*, 114(13):3521–3526, 2017. 2
- Kirsch, L., van Steenkiste, S., and Schmidhuber, J. Improving generalization in meta reinforcement learning using learned objectives. *arXiv preprint arXiv:1910.04098*, 2019. 2
- Koh, P. W., Sagawa, S., Marklund, H., Xie, S. M., Zhang, M., Balsubramani, A., Hu, W., Yasunaga, M., Phillips, R. L., Gao, I., et al. Wilds: A benchmark of in-the-wild distribution shifts. In *International Conference on Machine Learning*, pp. 5637–5664. PMLR, 2021. 2, 3, 4, 5, 6, 17, 18
- Krause, J., Stark, M., Deng, J., and Fei-Fei, L. 3d object representations for fine-grained categorization. In *Proceedings of the IEEE International Conference on Computer Vision Workshops*, pp. 554–561, 2013. 18
- Krizhevsky, A., Hinton, G., et al. Learning multiple layers of features from tiny images. 2009. 17
- Kumar, A., Raghunathan, A., Jones, R. M., Ma, T., and Liang, P. Fine-tuning can distort pretrained features and underperform out-of-distribution. In *International Conference on Learning Representations*, 2022a. 1, 3, 5, 16, 18
- Kumar, A., Shen, R., Bubeck, S., and Gunasekar, S. How to fine-tune vision models with sgd, 2022b. 2, 5, 6
- Lee, C., Cho, K., and Kang, W. Mixout: Effective regularization to finetune large-scale pretrained language models. *arXiv preprint arXiv:1909.11299*, 2019a. 2
- Lee, J., Tang, R., and Lin, J. What would elsa do? freezing layers during transformer fine-tuning. *arXiv preprint arXiv:1911.03090*, 2019b. 2
- Lee, Y., Chen, A. S., Tajwar, F., Kumar, A., Yao, H., Liang, P., and Finn, C. Surgical fine-tuning improves adaptation to distribution shifts. *arXiv preprint arXiv:2210.11466*, 2022a. 2, 3
- Lee, Y., Yao, H., and Finn, C. Diversify and disambiguate: Learning from underspecified data. *arXiv preprint arXiv:2202.03418*, 2022b. 3
- Li, D., Yang, Y., Song, Y.-Z., and Hospedales, T. Learning to generalize: Meta-learning for domain generalization. In *Proceedings of the AAAI conference on artificial intelligence*, volume 32, 2018a. 2
- Li, H., Chaudhari, P., Yang, H., Lam, M., Ravichandran, A., Bhotika, R., and Soatto, S. Rethinking the hyperparameters for fine-tuning. In *International Conference on Learning Representations*, 2020. 2
- Li, L., Jamieson, K., DeSalvo, G., Rostamizadeh, A., and Talwalkar, A. Hyperband: A novel bandit-based approach to hyperparameter optimization. *The journal of machine learning research*, 18(1):6765–6816, 2017. 2
- Li, L., Jamieson, K., Rostamizadeh, A., Gonina, E., Hardt, M., Recht, B., and Talwalkar, A. Massively parallel hyperparameter tuning. 2018b. 2, 5
- Lim, S., Kim, I., Kim, T., Kim, C., and Kim, S. Fast autoaugment. *Advances in Neural Information Processing Systems*, 32, 2019. 2
- Liu, E. Z., Haghighi, B., Chen, A. S., Raghunathan, A., Koh, P. W., Sagawa, S., Liang, P., and Finn, C. Just train twice: Improving group robustness without training group information. In *International Conference on Machine Learning*, pp. 6781–6792. PMLR, 2021a. 3
- Liu, H., Simonyan, K., and Yang, Y. Darts: Differentiable architecture search. *arXiv preprint arXiv:1806.09055*, 2018. 2
- Liu, Y., Agarwal, S., and Venkataraman, S. Autofreeze: Automatically freezing model blocks to accelerate fine-tuning. *arXiv preprint arXiv:2102.01386*, 2021b. 2
- Lu, S., Nott, B., Olson, A., Todeschini, A., Vahabi, H., Carmon, Y., and Schmidt, L. Harder or different? a closer look at distribution shift in dataset reproduction. In *ICML Workshop on Uncertainty and Robustness in Deep Learning*, volume 5, pp. 15, 2020. 5, 17
- Metz, L., Harrison, J., Freeman, C. D., Merchant, A., Beyer, L., Bradbury, J., Agrawal, N., Poole, B., Mordatch, I., Roberts, A., et al. Velo: Training versatile learned optimizers by scaling up. *arXiv preprint arXiv:2211.09760*, 2022. 2
- Miller, J. P., Taori, R., Raghunathan, A., Sagawa, S., Koh, P. W., Shankar, V., Liang, P., Carmon, Y., and Schmidt, L. Accuracy on the line: on the strong correlation between out-of-distribution and in-distribution generalization. In *International Conference on Machine Learning*, pp. 7721–7735. PMLR, 2021. 3

- Mukhoti, J., Gal, Y., Torr, P. H., and Dokania, P. K. Fine-tuning can cripple your foundation model; preserving features may be the solution. *arXiv preprint arXiv:2308.13320*, 2023. 3
- Oh, J., Hessel, M., Czarnecki, W. M., Xu, Z., van Hasselt, H. P., Singh, S., and Silver, D. Discovering reinforcement learning algorithms. *Advances in Neural Information Processing Systems*, 33:1060–1070, 2020. 2
- Oquab, M., Bottou, L., Laptev, I., and Sivic, J. Learning and transferring mid-level image representations using convolutional neural networks. In *Proceedings of the IEEE conference on computer vision and pattern recognition*, pp. 1717–1724, 2014. 2
- Qi, Q., Xu, Y., Jin, R., Yin, W., and Yang, T. Attentional biased stochastic gradient for imbalanced classification. *arXiv preprint arXiv:2012.06951*, 2020. 5
- Radford, A., Kim, J. W., Hallacy, C., Ramesh, A., Goh, G., Agarwal, S., Sastry, G., Askell, A., Mishkin, P., Clark, J., Krueger, G., and Sutskever, I. Learning transferable visual models from natural language supervision, 2021a. 18
- Radford, A., Kim, J. W., Hallacy, C., Ramesh, A., Goh, G., Agarwal, S., Sastry, G., Askell, A., Mishkin, P., Clark, J., et al. Learning transferable visual models from natural language supervision. In *International conference on machine learning*, pp. 8748–8763. PMLR, 2021b. 1, 3, 4, 5, 6, 18
- Ramasesh, V. V., Dyer, E., and Raghu, M. Anatomy of catastrophic forgetting: Hidden representations and task semantics. *arXiv preprint arXiv:2007.07400*, 2020. 2
- Real, E., Aggarwal, A., Huang, Y., and Le, Q. V. Regularized evolution for image classifier architecture search. In *Proceedings of the aaai conference on artificial intelligence*, volume 33, pp. 4780–4789, 2019. 2
- Recht, B., Roelofs, R., Schmidt, L., and Shankar, V. Do cifar-10 classifiers generalize to cifar-10? 2018. 5, 17
- Recht, B., Roelofs, R., Schmidt, L., and Shankar, V. Do imagenet classifiers generalize to imagenet? In *International Conference on Machine Learning*, pp. 5389–5400. PMLR, 2019. 5, 18
- Royer, A. and Lampert, C. A flexible selection scheme for minimum-effort transfer learning. In *Proceedings of the IEEE/CVF Winter Conference on Applications of Computer Vision*, pp. 2191–2200, 2020. 2
- Sagawa, S., Koh, P. W., Hashimoto, T. B., and Liang, P. Distributionally robust neural networks for group shifts: On the importance of regularization for worst-case generalization. *arXiv preprint arXiv:1911.08731*, 2019. 5
- Sagawa, S., Koh, P. W., Lee, T., Gao, I., Xie, S. M., Shen, K., Kumar, A., Hu, W., Yasunaga, M., Marklund, H., Beery, S., David, E., Stavness, I., Guo, W., Leskovec, J., Saenko, K., Hashimoto, T., Levine, S., Finn, C., and Liang, P. Extending the WILDS benchmark for unsupervised adaptation. In *International Conference on Learning Representations*, 2022. 18
- Salman, H., Ilyas, A., Engstrom, L., Kapoor, A., and Madry, A. Do adversarially robust imagenet models transfer better? *Advances in Neural Information Processing Systems*, 33:3533–3545, 2020. 3
- Sharif Razavian, A., Azizpour, H., Sullivan, J., and Carlsson, S. Cnn features off-the-shelf: an astounding baseline for recognition. In *Proceedings of the IEEE conference on computer vision and pattern recognition workshops*, pp. 806–813, 2014. 2
- Shen, Z., Liu, Z., Qin, J., Savvides, M., and Cheng, K.-T. Partial is better than all: Revisiting fine-tuning strategy for few-shot learning. In *Proceedings of the AAAI Conference on Artificial Intelligence*, volume 35, pp. 9594–9602, 2021. 2
- Taori, R., Dave, A., Shankar, V., Carlini, N., Recht, B., and Schmidt, L. Measuring robustness to natural distribution shifts in image classification. *Advances in Neural Information Processing Systems*, 33:18583–18599, 2020. 3, 5
- Tian, J., He, Z., Dai, X., Ma, C.-Y., Liu, Y.-C., and Kira, Z. Trainable projected gradient method for robust fine-tuning. In *Proceedings of the IEEE/CVF Conference on Computer Vision and Pattern Recognition*, pp. 7836–7845, 2023. 2
- Torralba, A., Fergus, R., and Freeman, W. T. 80 million tiny images: A large data set for nonparametric object and scene recognition. *IEEE Transactions on Pattern Analysis and Machine Intelligence*, 30(11):1958–1970, 2008. 5, 17
- Touvron, H., Cord, M., El-Nouby, A., Verbeek, J., and Jégou, H. Three things everyone should know about vision transformers. *arXiv preprint arXiv:2203.09795*, 2022. 2
- Tzeng, E., Hoffman, J., Zhang, N., Saenko, K., and Darrell, T. Deep domain confusion: Maximizing for domain invariance. *arXiv preprint arXiv:1412.3474*, 2014. 3
- Veeling, B. S., Linmans, J., Winkens, J., Cohen, T., and Welling, M. Rotation equivariant cnns for digital pathology. *arXiv preprint arXiv:1806.03962*, 2018. 18

- Wang, H., Ge, S., Lipton, Z., and Xing, E. P. Learning robust global representations by penalizing local predictive power. In *Advances in Neural Information Processing Systems*, pp. 10506–10518, 2019. [5](#), [18](#)
- Wichrowska, O., Maheswaranathan, N., Hoffman, M. W., Colmenarejo, S. G., Denil, M., de Freitas, N., and Sohl-Dickstein, J. Learned optimizers that scale and generalize. 2017. [2](#)
- Wiles, O., Gowal, S., Stimberg, F., Alvisè-Rebuffi, S., Ktena, I., Cemgil, T., et al. A fine-grained analysis on distribution shift. *arXiv preprint arXiv:2110.11328*, 2021. [3](#)
- Wortsman, M., Ilharco, G., Gadre, S. Y., Roelofs, R., Gontijo-Lopes, R., Morcos, A. S., Namkoong, H., Farhadi, A., Carmon, Y., Kornblith, S., et al. Model soups: averaging weights of multiple fine-tuned models improves accuracy without increasing inference time. In *International Conference on Machine Learning*, pp. 23965–23998. PMLR, 2022a. [3](#), [6](#)
- Wortsman, M., Ilharco, G., Kim, J. W., Li, M., Kornblith, S., Roelofs, R., Lopes, R. G., Hajishirzi, H., Farhadi, A., Namkoong, H., et al. Robust fine-tuning of zero-shot models. In *Proceedings of the IEEE/CVF Conference on Computer Vision and Pattern Recognition*, pp. 7959–7971, 2022b. [1](#), [3](#), [5](#), [6](#), [7](#), [15](#), [16](#), [18](#)
- Xu, Y., Xie, L., Zhang, X., Chen, X., Qi, G.-J., Tian, Q., and Xiong, H. Pc-darts: Partial channel connections for memory-efficient architecture search. *arXiv preprint arXiv:1907.05737*, 2019. [2](#)
- Xuhong, L., Grandvalet, Y., and Davoine, F. Explicit inductive bias for transfer learning with convolutional networks. In *International Conference on Machine Learning*, pp. 2825–2834. PMLR, 2018. [2](#), [3](#)
- Yao, H., Wang, Y., Li, S., Zhang, L., Liang, W., Zou, J., and Finn, C. Improving out-of-distribution robustness via selective augmentation. In *International Conference on Machine Learning*, pp. 25407–25437. PMLR, 2022. [5](#)
- Yosinski, J., Clune, J., Bengio, Y., and Lipson, H. How transferable are features in deep neural networks? *Advances in neural information processing systems*, 27, 2014. [2](#)
- Yu, T., Finn, C., Xie, A., Dasari, S., Zhang, T., Abbeel, P., and Levine, S. One-shot imitation from observing humans via domain-adaptive meta-learning. *arXiv preprint arXiv:1802.01557*, 2018. [2](#)
- Zhang, J. O., Sax, A., Zamir, A., Guibas, L., and Malik, J. Side-tuning: a baseline for network adaptation via additive side networks. In *European Conference on Computer Vision*, pp. 698–714. Springer, 2020. [2](#)
- Zhang, M., Marklund, H., Dhawan, N., Gupta, A., Levine, S., and Finn, C. Adaptive risk minimization: Learning to adapt to domain shift. *Advances in Neural Information Processing Systems*, 34:23664–23678, 2021. [2](#)
- Zoph, B. and Le, Q. V. Neural architecture search with reinforcement learning. *arXiv preprint arXiv:1611.01578*, 2016. [2](#)
- Zoph, B., Vasudevan, V., Shlens, J., and Le, Q. V. Learning transferable architectures for scalable image recognition. In *Proceedings of the IEEE conference on computer vision and pattern recognition*, pp. 8697–8710, 2018. [2](#)

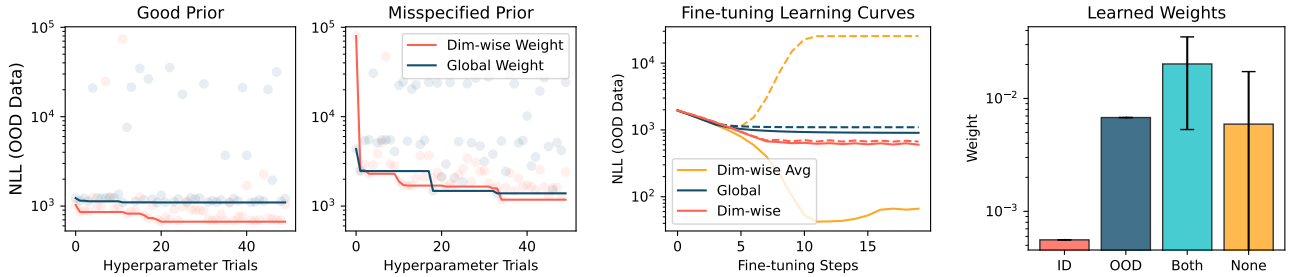


Figure 6: **Didactic experiment.** *Left two:* learning curves for fitting a Gaussian distribution to toy data. Hyperparameter optimization with a larger hyperparameter space (red) leads to better OOD performance only when the prior is informative. *Right:* fine-tuning learning curves with learned hyperparameters. Averaging the dimension-wise weights (yellow) results in massively overfitting to the ID data (solid) and underperforming OOD (dashed). The dimension-wise hyperparameters (red) show the best generalization. *Far right:* visualization of learned loss weights w_i for each dimension. The learned weights are lowest for the dimensions where ID alone differs from the prior (red), indicating that the model learns to ignore the ID data in these dimensions.

A Intuition and Didactic Experiment for AUTOFT

To illustrate how hyperparameter optimization can lead to more effective adaptation of a partially useful prior, we consider a simple experiment. We focus on synthetic datasets of vectors drawn from zero-mean Gaussian distributions with different variances.

We assume that the prior unit variance distribution is helpful but that the data exhibits deviation from this prior along a few dimensions. The prior distribution is a unit Gaussian, i.e., it has variance $[1.0, 1.0, \dots]$. Training data D_{tr} is drawn from a distribution with variance $[10^{-3}, 10^{-3}, 10^{-3}, 10^{-3}, 1.0, 1.0, \dots]$, while the validation data D_{val} is drawn from a distribution with variance $[10^{-3}, 10^{-3}, 10^{-3}, 1.0, 10^{-3}, 1.0, \dots]$. We fit the parameters of a Gaussian distribution q_θ to the training data using a variational Bayes objective by minimizing the following loss:

$$\arg \min_{\theta} D_{KL}(q_\theta || p) + \sum_{i=1}^{10} w_i \text{NLL}_i(q_\theta, \mathcal{D}). \quad (2)$$

We consider “fine-tuning” as starting from the prior distribution. In this toy model, dimension-wise weight hyperparameters w_i dictate the degree of influence of the prior versus the training data on each dimension, analogous to how the fine-grained hyperparameters in AUTOFT balance the foundation model prior and training data along different aspects of fine-tuning. As in AUTOFT, we use the TPE algorithm to optimize the weight hyperparameters w_i to maximize the log-likelihood of the validation data D_{val} .

Results in Figure 6 show the effect of standard hyperparameter tuning (global weight) versus considering an expanded hyperparameter space as in AUTOFT (dim-wise weight). Learning dimension-wise weights is effective, but only when the prior distribution is well-specified and provides a better signal for OOD generalization than the training set along some dimensions, as foundation models do for general fine-tuning tasks. This additional expressivity is necessary to specify a better adaptation procedure: naively averaging the learned dim-wise parameters causes the model to overfit the ID data. Finally, through inspecting the learned weights, we see that the learned dim-wise weights improve OOD generalization by downweighting the influence of the ID data in the directions where only the ID data differs from the prior (not the OOD data).

B Additional Results

B.1 ImageNet Distribution Shifts

B.1.1 MAIN RESULTS

We provide detailed results for each ImageNet-derived distribution shift in Table 9. AutoFT outperforms all baselines on 9 out of 10 OOD datasets. AUTOFT improves OOD performance by 3.0% compared to the leading baseline, FLYP. We observe a similar effect with all other points of comparison, suggesting that perhaps these prior methods for robust fine-tuning “overfit” to the ID distribution in a way that AUTOFT does not.

| Methods | Without Ensembling | | | | | | | With Ensembling | | | | | | |
|---------------|--------------------|-------------|-------------|-------------|-------------|-------------|-------------|-----------------|-------------|-------------|-------------|-------------|-------------|-------------|
| | ID | Im-V2 | Im-R | Im-A | Sketch | ObjectNet | Avg. OOD | ID | Im-V2 | Im-R | Im-A | Sketch | ObjectNet | Avg. OOD |
| Zeroshot | 68.3 | 61.9 | 77.7 | 50.0 | 48.3 | 55.4 | 58.7 | 68.3 | 61.9 | 77.7 | 50.0 | 48.3 | 55.4 | 58.7 |
| LP | 79.9 | 69.8 | 70.8 | 46.4 | 46.9 | 52.1 | 57.2 | 80.0 | 70.3 | 72.4 | 47.8 | 48.1 | 52.8 | 58.3 |
| FT | 81.3 | 71.2 | 66.1 | 37.8 | 46.1 | 53.3 | 54.9 | 82.5 | 72.8 | 74.9 | 48.1 | 51.9 | 59.0 | 61.3 |
| L2-SP | 81.7 | 71.8 | 70.0 | 42.5 | 48.5 | 56.2 | 57.8 | 82.2 | 72.9 | 75.1 | 48.6 | 51.4 | 58.9 | 61.4 |
| LP-FT | 81.7 | 72.1 | 73.5 | 47.6 | 50.3 | 58.2 | 60.3 | 82.1 | 72.8 | 75.3 | 50.1 | 51.7 | 59.2 | 61.8 |
| FLYP | 82.6 | 73.0 | 71.4 | 48.1 | 49.6 | 58.7 | 60.2 | 82.9 | 73.5 | 76.0 | 53.0 | 52.3 | 60.8 | 63.1 |
| AUTOFT | 81.8 | 73.1 | 72.4 | 48.8 | 49.8 | 63.5 | 61.5 | 82.4 | 73.6 | 76.4 | 53.1 | 52.6 | 65.6 | 64.3 |

Table 9: **Detailed ImageNet results.** AUTOFT consistently outperforms all baselines on 9 out of 10 ImageNet distribution shifts.

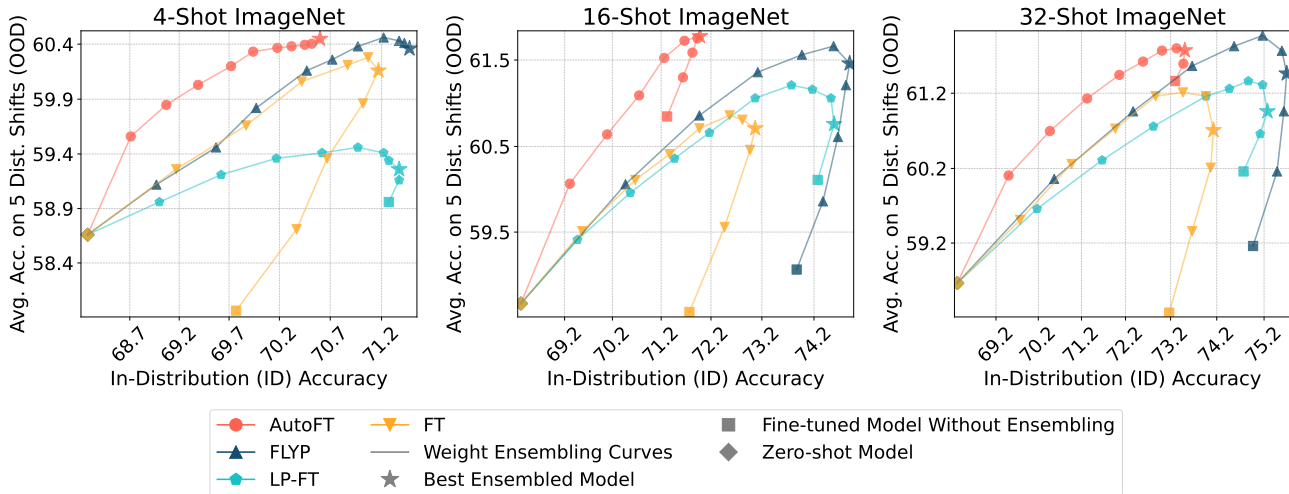


Figure 7: **AUTOFT improves OOD generalization in few-shot learning.** AUTOFT results in gains in *effective robustness* over baselines, indicated by vertical distance. AUTOFT results in better OOD performance at a given ID performance threshold across varying degrees of weight interpolation between the fine-tuned and zero-shot models.

| Methods | CalTech-101 | Stanford Cars | Flowers-102 |
|---------------|-------------------|-------------------|-------------------|
| Zeroshot | 87.7 (-) | 64.4 (-) | 71.2 (-) |
| LP | 94.8 (0.0) | 83.1 (0.0) | 95.9 (0.0) |
| FT | 97.2 (0.1) | 84.4 (0.3) | 90.4 (0.5) |
| LP-FT | 96.9 (0.6) | 89.4 (0.1) | 97.9 (0.1) |
| FLYP | 97.6 (0.1) | 89.6 (0.3) | 97.7 (0.1) |
| AUTOFT | 99.0 (0.1) | 89.6 (0.2) | 97.6 (0.2) |

Table 10: **AUTOFT can lead to improvements in IID transfer learning.** In addition to enhancing OOD generalization, AUTOFT can improve performance in IID transfer learning settings when using an ID validation set to learn the objective and hyperparameters..

B.1.2 FEW-SHOT CLASSIFICATION

Figure 7 plots effective robustness at varying interpolation coefficients on five ImageNet distribution shifts for 4, 16, and 32 shot classification. In all three settings, AUTOFT results in better OOD generalization and avoids overfitting to the small fine-tuning dataset. For example, in 32-shot ImageNet, AUTOFT improves average OOD accuracy by 2.2% compared to the leading baseline, FLYP.

B.2 CIFAR-10 Distribution Shifts

AUTOFT also outperforms prior robust fine-tuning approaches on the subtle CIFAR-10.1 and CIFAR-10.2 distribution shifts. Here, AUTOFT uses the CLIP ViT-L/14 backbone, following Wortsman et al. (2022b), and 100 examples from CIFAR-10-C

| Method | CIFAR-10.1 | CIFAR-10.2 |
|--|-------------|-------------|
| Zero-shot | 92.5 | 88.8 |
| Fine-tuning | 95.9 | 91.3 |
| AUTOFT | 97.5 | 93.5 |
| WiSE-FT (best α) | 98.0 | 94.4 |
| AUTOFT (best α) | 98.3 | 95.0 |

Table 11: **Evaluation on CIFAR-10 distribution shifts.** AUTOFT outperforms fine-tuning by 2.2% on CIFAR-10.2 and by 1.4% on CIFAR-10.1, using only 100 samples from CIFAR-10-C. AUTOFT additionally outperforms WiSE-FT with weight ensembling.

| iWildCam | | |
|------------------|-------------|-------------|
| Method | ID | OOD |
| AUTOFT | 51.0 | 38.3 |
| Layerwise AUTOFT | 47.8 | 34.6 |

Table 12: **Expressivity of the AUTOFT search space.** AUTOFT results in better performance than its layerwise variant with per-layer learning rates, weight decays, and L1/L2 distances to pretrained parameters. Evaluation is on the iWildCam benchmark. This suggests that more expressive hyperparameter spaces overfit to the validation set, degrading performance.

to learn the fine-tuning objective and hyperparameters.

C Additional Experiments

C.1 Expressivity of Hyperparameter Space

We investigate whether more expressive hyperparameter search spaces result in better performance. We compare AUTOFT against a layerwise variant of AUTOFT that learns per-layer learning rates, weight decays, and L1/L2 norms and regularization terms in Table 12. The layerwise variant of AUTOFT results in worse ID and OOD performance, suggesting that an overly expressive search space leads to overfitting of the small validation set.

D Experimental Details

D.1 Training Protocol

We closely follow the training details of Goyal et al. (2022a) and Wortsman et al. (2022b). All methods fine-tune models with an AdamW optimizer, cosine learning rate scheduler, and a batch size of 512 for ImageNet and 256 for all other datasets. All baseline hyperparameters, such as learning rate, weight decay, and warmup length, are tuned through grid search. All methods, including AUTOFT, perform early stopping based on in-distribution (ID) validation accuracy. We provide a comprehensive breakdown of the hyperparameter sweeps in the supplementary material. We emphasize that none of these methods, including AUTOFT, observe any of the test OOD distributions during training. Finally, we report metrics averaged over 5 runs with 95% confidence intervals.

D.2 Baselines

We follow the training details in Goyal et al. (2022a). For all datasets excluding ImageNet, we use a batch size of 256 and conduct a hyperparameter sweep across five learning rates $\{10^{-6}, 10^{-5}, \dots, 10^{-2}\}$ and five weight decay values in the range $\{0.0, 0.1, \dots, 0.4\}$. On ImageNet, we use a larger batch size of 512 and perform a hyperparameter sweep over three learning rates $\{10^{-6}, 10^{-5}, 10^{-4}\}$ and two weight decays $\{0, 0.1\}$. For L2-SP, we tune the weight of the regularization term $\lambda \in \{10^{-4}, 10^{-3}, 10^{-2}, 10^{-1}\}$. We select baseline hyperparameters based on ID validation performance. For datasets without a standard validation set, we split the training data into an 80:20 ratio to create one.

D.3 AUTOFT

Hyperparameter search space. As described in Section 4, AUTOFT learns weights for nine different losses on a log-uniform range $[10^{-4}, 10]$. AUTOFT additionally searches for learning rate in the log-uniform range $[10^{-2} \cdot \eta^*, 10^2 \cdot \eta^*]$, where η^* is the conventional learning rate used in prior works on fine-tuning (Wortsman et al., 2022b; Kumar et al., 2022a;

Goyal et al., 2022a), weight decay values in the log-uniform range $[0.0, 1.0]$, and random seeds in the range $[0, 100]$. The layerwise variant of AUTOFT learns per-layer learning rates and weight decay regularization terms, each sampled from the same respective range.

WILDS-iWildCam and WILDS-FMoW state-of-the-art (SoTA). For the iWildCam and FMoW SoTA results in Table 2, we fine-tune the ViT-L/14@336px model with loss weights learned on the smaller ViT-B/16 backbone with AUTOFT. Applying AUTOFT directly to the ViT-L/14@336px model may improve performance further, although at the cost of more compute.

Validation sets. For the iWildCam and FMoW experiments, we use 1000 examples from the official WILDS OOD validation splits from Koh et al. (2021). For ImageNet, we use 1000 examples from ImageNet-C. For CIFAR-10, we use 100 examples from CIFAR-10-C. For the few-shot experiments, we use a randomly sampled k -shot ID validation set, and average over 50 runs to account for variance in the fine-tuning and validation sets. For the transfer learning experiments, we *do not use OOD data*. We randomly partition the ID validation sets into two validation sets: one for hyperparameter optimization, and the other for early stopping during final fine-tuning. We use 100, 200, 400 examples for Caltech-101, Stanford Cars, and Flowers-102, respectively.

Hyper-hyperparameters. We list hyper-hyperparameters used in Table 1. Few-shot hyper-hyperparameters are listed in Table 13. We run AUTOFT with 500 outer-loop trials on all non-few shot experiments, which is the largest number of trials that can be run with a reasonable amount of compute. We use grid-search to tune the number of inner steps and validation set size and select hyper-hyperparameters based on ID validation performance of the final fine-tuned model. On iWildCam, FMoW, and CIFAR-10, we tune over $\{10, 50, 100\}$ inner steps and $\{100, 1000, 5000\}$ validation examples. On ImageNet, we tune over $\{10, 50\}$ inner steps and $\{1000, 5000\}$ validation examples. On Caltech-101, Stanford Cars, and Flowers-102, we tune over $\{10, 50\}$ inner steps. For the few-shot binary classification experiments, we run AUTOFT with 50 outer-loop evaluations and tune over $\{5, 10, 20\}$ inner steps. For the few-shot ImageNet experiments, we run AUTOFT with 100 outer-loop evaluations and tune over $\{5, 20, 50\}$ inner steps.

Our empirical results show that a small number of inner loop steps is effective for identifying suitable hyperparameters. This is also a necessity considering computational constraints. Our method strikes a balance between practical feasibility and reliable hyperparameter selection.

Few-shot classification. In the k -shot setting with $k \in \{4, 16, 32\}$, we select k training and k validation examples from each class. To account for variance from the small training and validation sets, for each run of AUTOFT, we repeat hyperparameter optimization 5 times and select the best set of hyperparameters based on ID validation performance. We then average results over 50 runs.

Transferability of learned hyperparameters experiment details. The OOD distributions for fine-tuning on CIFAR-10 are CIFAR-10.1 and CIFAR-10.2. The OOD distributions for fine-tuning on MNIST are MNIST-C, rotated MNIST, colored MNIST, and EMNIST.

D.4 Datasets

Below, we summarize the datasets we use for evaluation, including the fine-tuning dataset (ID), the validation dataset for hyperparameter optimization, and the test OOD datasets.

- **CIFAR-10** (Krizhevsky et al., 2009) contains 60,000 images across 10 classes. We use CIFAR-10 for fine-tuning, 100 examples from CIFAR-10-C for validation, and the CIFAR-10.1 (Recht et al., 2018; Torralba et al., 2008) and CIFAR-10.2 (Lu et al., 2020) as OOD test sets.

| Dataset | Steps | Trials |
|---------------|-------|--------|
| SST-2 | 10 | 50 |
| PatchCamelyon | 10 | 50 |
| ImageNet-4 | 5 | 100 |
| ImageNet-16 | 20 | 100 |
| ImageNet-32 | 50 | 100 |

Table 13: AUTOFT training settings for few-shot classification experiments.

- **ImageNet** (Deng et al., 2009) contains over a million images in 1000 categories. We use ImageNet as our ID distribution, 15000 examples from ImageNet-C for validation, and five ImageNet variations for the OOD datasets following prior works (Radford et al., 2021a; Wortsman et al., 2022b; Kumar et al., 2022a; Goyal et al., 2022a): ImageNet-V2 (Recht et al., 2019), ImageNet-R (Hendrycks et al., 2021a), ImageNet-A (Hendrycks et al., 2021b), ImageNet-Sketch (Wang et al., 2019), and ObjectNet (Barbu et al., 2019).
- **WILDS-iWildCam** (Beery et al., 2021; Koh et al., 2021; Sagawa et al., 2022) is an animal camera trap image classification dataset where the label y is one of 182 animal species. The ID and OOD datasets consist of photos from disjoint sets of camera traps, making the images differ in camera specifications and attributes such as background and lighting. We use the official splits from Koh et al. (2021) and use the ID train set for fine-tuning, the OOD validation set for hyperparameter optimization, and the OOD test set for evaluation.
- **WILDS-FMoW** (Christie et al., 2018; Koh et al., 2021; Sagawa et al., 2022) contains remote sensing imagery from satellites. Each image is to be classified into one among 62 categories, including labels like “impoverished settlement” and “hospital.” The ID and OOD datasets differ in year of acquisition and geographic location. We use the official splits from Koh et al. (2021) and use the ID train set for fine-tuning, the OOD validation set for hyperparameter optimization, and the OOD test set for evaluation.

In all of the transfer learning datasets described below, we use a subset of the ID validation set for hyperparameter optimization. In other words, we do not use an “OOD” validation set.

- **Caltech101** (Fei-Fei et al., 2004) contains images of objects from 101 different categories, including “dragonfly,” “grand piano,” and “saxophone.”
- **StanfordCars** (Krause et al., 2013) features a collection of car images categorized by model, make, and year, where the task is to classify them into one of 196 types, such as “Ford Mustang Convertible 1967” or “Toyota Prius Hatchback 2009.”
- **Flowers102** (Veeling et al., 2018) consists of flower images from the UK, with the objective of classifying each image into one of 102 species, such as “oxeye daisy” or “hibiscus.”
- **PatchCamelyon** (Veeling et al., 2018) provides digital pathology images for binary classification, with the goal of identifying metastatic tumor tissues.
- **Rendered SST2** (Radford et al., 2021b) is a dataset for optical character recognition, where the task is to classify text sentiment as “positive” or “negative.”